Synthesis and DNA-binding properties of bisdiazoliumylporphyrins

Daryono H. Tjahjono,* Tomoko Yamamoto, Sumito Ichimoto, Naoki Yoshioka and Hidenari Inoue

Department of Applied Chemistry, Keio University, 3-14-1 Hiyoshi, Kohoku-ku, Yokohama 223-8522, Japan. E-mail: c02935@educ.cc.keio.ac.jp

Received (in Cambridge, UK) 7th July 2000, Accepted 26th July 2000
Published on the Web 29th August 2000

A pair of 5,15-bisdiazoliumylporphyrins with only two *meso*-substituents, 5,15-bis(1,3-dimethylimidazolium-2-yl)-porphyrin **1b** and 5,15-bis(1,2-dimethylpyrazolium-4-yl)porphyrin **2b**, has been synthesized. The crowded porphyrin **1b** intercalates between base pairs of DNA to stabilize the duplex DNA to thermal denaturation due to its high affinity for DNA. The binding of porphyrin **1b** to DNA is an exothermic interaction and enthalpically driven. Porphyrin **1b** interacts more strongly with poly(dA-dT)$_2$ than with poly(dG-dC)$_2$, and the interaction is more favorable or selective to AT-rich sites than to GC-rich sites.

Introduction

Cationic porphyrins and their non-covalent interactions with DNA are of interest from the viewpoint of their role in biological systems. It has been reported that they act as an inhibitor of human telomerases,[1] a receptor for peptides[2] and a DNA cleaver.[3] Except for the experimental conditions such as pH, ionic strength and molar ratio of porphyrin to DNA base pair,[4–6] the nature of porphyrins plays an important role in their binding to DNA. Therefore, the design and synthesis of cationic porphyrins as well as their interaction with DNA are interesting challenges. So far, *meso*-tetrakis(*N*-methylpyridinium-4-yl)porphyrin (H_2TMPyP) and its derivatives are well known as cationic porphyrins with six-membered rings at the *meso*-position.[1–7]

Three major binding modes have been proposed for cationic porphyrin binding to DNA: intercalation and two types of outside binding. The first type is the outside binding involving both placement of porphyrin in the minor groove and electronic interaction with the phosphate backbone, and the second type is the stacking of the porphyrin along the DNA helix.[4,5] The binding of porphyrin to DNA is presumably stabilized by electronic interactions between the positively charged substituents on the porphyrin periphery and the negatively charged phosphate oxygen atom of DNA. In the case of intercalation, favorable aromatic π–π stacking interactions between the porphyrin macrocycle and nucleic acid bases are also involved.[7]

The porphyrin core is planar but it is shielded by peripheral substituents. This makes cationic porphyrins different from conventional intercalators such as ethidium bromide, proflavin and daunomycin in which the planar fused-aromatic ring can slip between adjacent base pairs of DNA without requiring any major distortion from the idealized B-DNA form. A study of cationic porphyrin–DNA interaction in solution shows that intercalation of porphyrin into DNA requires conformational distortion of DNA, but the base pairs flanking the binding site are not disrupted.[7] In general, intercalation of cationic porphyrin into DNA shows a higher binding constant than that of outside binding.[5] Recently, we have reported that cationic porphyrins with five-membered rings as *meso*-substituents interact with DNA, but their DNA-binding properties are different from those of the well known H_2TMPyP because of the differences in charge distribution of the *meso*-substituent and electronic density of the porphyrin core.[8] In the present study, cationic porphyrins with only two diazolium rings at the 5- and 15-positions have been synthesized. The absence of two *meso*-substituents in *trans* positions was expected to drive the intercalation of these cationic porphyrins into the DNA base pairs. The following results have revealed that the elimination of two *meso*-substituents from tetrakis(dimethylimidazoliumyl)porphyrin dramatically changes its DNA-binding properties.

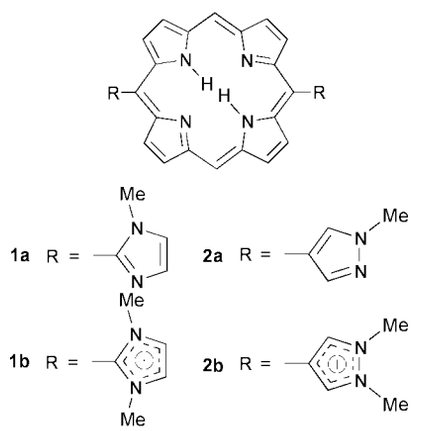

Fig. 1 Structure of 5,15-bisdiazoliumylporphyrins.

Results and discussion

A. Synthesis of porphyrins and their solution characteristics

Non-cationic 5,15-bis(1-methylimidazol-2-yl)porphyrin **1a** and 5,15-bis(1-methylpyrazol-4-yl)porphyrin **2a** were synthesized by the Lindsey method.[9] Reaction of **1a** with a large excess (≈250 equiv.) of iodomethane afforded dicationic **1b** in moderate yield (90%). Dicationic **2b** was obtained by stirring **2a** with an excess (≈20 equiv.) of methyl fluorosulfonate (Fig. 1). Both **1b** and **2b** are freely soluble in water. However, a further investigation of their solution characteristics showed that **2b** is self-stacked in aq. sodium chloride (0.01 M). An adoption of the dimerization model[10] confirmed that **2b** is dimerized in aq. sodium chloride (0.1 M). This dimerization of **2b** is an exothermic interaction and depends on the temperature (Fig. 2). It was also found that, in the temperature range 10–40 °C, the enthalpy and entropy changes in the dimerization of **2b** are −78.3 kJ mol^{-1} and −169.2 J K^{-1} mol^{-1}, respectively. In

DOI: 10.1039/b005491g

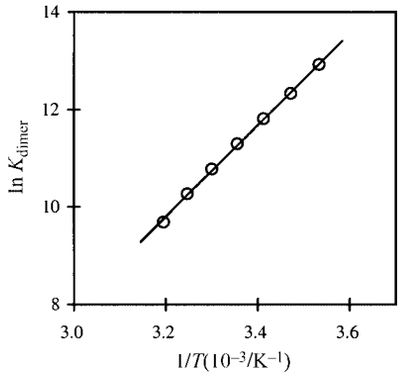

Fig. 2 Temperature dependence of the dimerization constant (K_{dimer}) of the porphyrin **2b** in phosphate buffer (pH 6,8, $\mu = 0.1$ M).

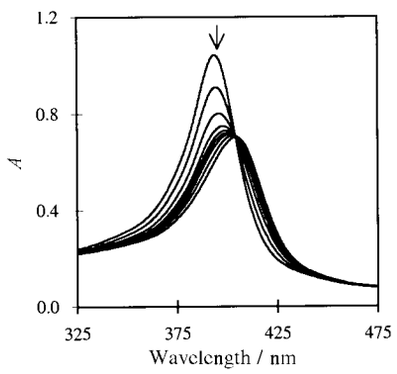

Fig. 3 Visible spectral changes of 7.84 μM **1b** upon addition of CTDNA. The direction of the arrow corresponds to decreasing *R*-values (∞, 0.85, 0.28, 0.21, 0.17, 0.12, 0.08, 0.04, 0.02).

contrast, **1b** neither dimerizes nor aggregates even in conc. aq. sodium chloride (2.0 M). This suggests that π–π interaction between porphyrin molecules does not occur in **1b** because cofacial interaction is suppressed in the presence of the dimethyl groups on the imidazolium rings. Therefore, porphyrin–DNA interaction has been studied only in **1b**, in which no stacking problem arises unlike in **2b**.

B. DNA-binding modes of porphyrins

In the presence of calf thymus DNA (CTDNA), the Soret band of **1b** showed a large red shift (12 nm) and substantial hypochromicity (34%) and finally changed to a new single peak at 406 nm at *R* (= [porphyrin]/[DNA base-pair])-values of 0.02 and lower (Fig. 3). At these *R*-values the induced CD spectra of **1b** appeared as a weak conservative signal (see Fig. 6) of a pattern very similar to that of H_2TMPyP.[5,8] This CD spectral frame suggests that **1b** is intercalated into CTDNA although the intercalation is probably accompanied by outside binding. Furthermore, an application of the CD matrix method (CD-mm)[11] to the observed induced CD spectra has revealed that **1b** is intercalated between GC and AT base pairs of CTDNA. The interaction of **1b** with DNA was also investigated using the synthetic polynucleotides poly(dG-dC)$_2$ and poly(dA-dT)$_2$. The shift (nm) and hypochomicity (%) in the Soret band at $R = 0.02$ are 11 nm and 51% for poly(dG-dC)$_2$ and 15 nm and 37% for poly(dA-dT)$_2$ as shown in Fig. 4 and Fig. 5, respectively. In the induced CD spectra a single negative signal was observed at 405 nm for **1b** bound to poly(dG-dC)$_2$ while a single positive signal appeared at 410 nm in that bound to poly(dA-dT)$_2$ (Fig. 6). On the basis of the observed visible spectra and the application of CD-mm assignments[11] to the observed CD spectra, it has been confirmed that **1b** is intercalated into both poly(dG-dC)$_2$ and poly(dA-dT)$_2$. In the case of intercalation of **1b** into the base-pair, one of the positively charged *N*,*N*′-

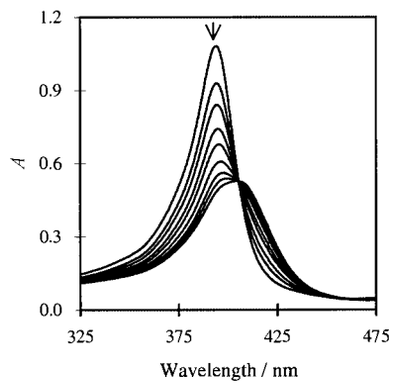

Fig. 4 Visible spectral changes of 8.14 μM **1b** upon addition of poly(dG-dC)$_2$. The direction of the arrow corresponds to decreasing *R*-values (∞, 0.80, 0.20, 0.11, 0.08, 0.05, 0.04, 0.03, 0.02).

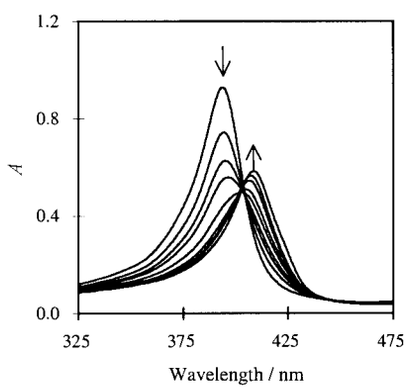

Fig. 5 Visible spectral changes of 6.99 μM **1b** upon addition of poly(dA-dT)$_2$. The direction of the arrow corresponds to decreasing *R*-values (∞, 0.85, 0.28, 0.21, 0.17, 0.12, 0.08, 0.04, 0.02).

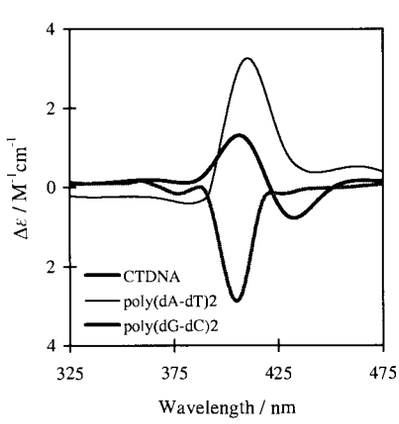

Fig. 6 Induced CD spectra of **1b** upon interaction with DNA at $R = 0.02$, in phosphate buffer (pH 6.8, $\mu = 0.2$ M).

dimethylimidazolium rings is located in the minor groove near the phosphate backbone and the other is placed in the major groove near the other phosphate backbone. These spectroscopic findings are in contrast to those in the parent tetracationic *meso*-tetrakis(1,3-dimethylimidazolium-2-yl)porphyrin (H_2TDMImP) which is bound to the outside of CTDNA.[8] In fact, H_2TDMImP hardly interacts with poly(dG-dC)$_2$ at all, giving rise to no induced CD band, and exhibits neither hypochromicity nor any shift in the Soret band, while it interacts with poly(dA-dT)$_2$ as an outside binder and undergoes changes in the visible absorption and induced CD spectra very similar to those in CTDNA.

In the absence of X-ray structural data, hydrodynamic methods which are sensitive to changes in the length of DNA are arguably the most critical test of the classical intercalation

model, and therefore they provide the most definitive means of inferring the binding mode of DNA in solution.[12] For this reason, the above unexpected results were clarified by examination of the interactions by viscometric measurements. The viscosity of buffer solutions of CTDNA and poly(dA-dT)$_2$ was increased with increasing addition of **1b** (Fig. 7). Such an increase in the relative viscosity is ascribed to a length increase of the DNA helix due to the intercalation. These results are consistent with the conclusion drawn from the visible and induced CD spectra that **1b** intercalates into CTDNA and poly(dA-dT)$_2$. Thus, **1b**, *i.e.* a cationic porphyrin bearing two crowded dimethylimidazolium groups at the *trans-meso*-positions, intercalates into the DNA base pairs if there are no substituents at the other two *trans-meso*-positions.

C. Thermodynamics of the porphyrin–DNA interaction

The peculiar interaction of **1b** with DNA was further studied by measuring the changes in the melting temperature (T_m) of double-helix DNA upon increasing addition of **1b** to the phosphate buffer of DNA. Plots of the increase in DNA melting temperature (ΔT_m) *versus* R of **1b** are shown in Fig. 8. The T_m of CTDNA increased with increasing addition of **1b** and increased even more by the addition of tetracationic H_2TDMImP.[8] The T_m of both poly(dA-dT)$_2$ and poly(dG-dC)$_2$ also increased upon addition of **1b**. The T_m profile of DNA is sensitive to its double-helix stability and binding of compounds to DNA alters the T_m depending on the strength of interactions. Therefore, it can be used as an indicator of binding properties of porphyrins to DNA and also of their binding strength. Thus, the above results indicated that **1b** interacts strongly with both natural and synthetic DNA to stabilize the duplex DNA to thermal denaturation.

Other evidence for the strong interaction of **1b** with DNA is that the apparent binding constant of **1b** to CTDNA is comparable to that of the well known intercalator H_2TMPyP, and is much larger than that of the outside binder H_2TDMImP. The binding constants of **1b**, H_2TMPyP and H_2TDMImP to CTDNA are 2.26×10^6 M^{-1}, 1.16×10^6 M^{-1} and 4.22×10^4 M^{-1}, respectively in phosphate buffer solution (pH 6.8; $\mu = 0.2$ M; 25 °C). A more detailed study of DNA binding of **1b** has revealed that **1b** is bound more tightly to poly(dA-dT)$_2$ (10^7 M^{-1}) than to poly(dG-dC)$_2$ (10^5 M^{-1}) (Table 1). These binding constants are extremely large at moderate ionic strengths and do not vary as linearly with decrease in the charge number as those observed for H_2TMPyP derivatives.[13] The high affinity of **1b** to DNA is probably associated with an increase in lipophilicity of the porphyrin with a lower cationic charge.

Finally, the thermodynamics of the interaction of **1b** with DNA was investigated in order to understand the molecular forces of complex formation between cationic porphyrins and DNA. In this case, the thermodynamics of the porphyrin–DNA interaction was studied in terms of the values of the binding constants determined at various temperatures. This approach provides a good means to indirectly determine the thermodynamic parameters of porphyrin–DNA interaction by the van't Hoff plot over a certain temperature range. Our linear van't Hoff plots indicated that no change in heat capacity occurred over the temperature range 18–39 °C. Thus, values for ΔG, ΔH and ΔS obtained serve as thermodynamic parameters of the porphyrin **1b**–DNA interaction (Table 1). It has been revealed that the standard free-energy changes for porphyrin **1b**–DNA interaction are large and negative and thus their association is strong. It has also been indicated that the binding of porphyrin **1b** to each DNA is an exothermic interaction.

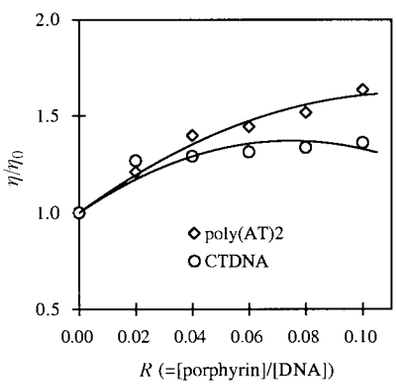

Fig. 7 Plots of the relative viscosity of DNA *versus* R of **1b** in phosphate buffer (pH 6.8, $\mu = 0.2$ M) at 30 ± 1 °C.

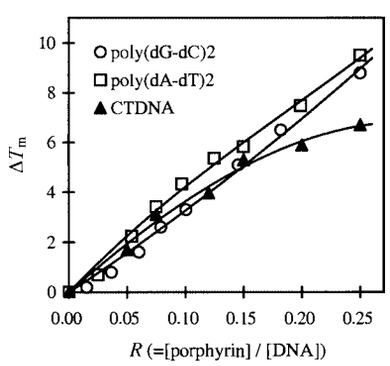

Fig. 8 Plots of the increase in DNA melting temperature (ΔT_m) *versus* R of **1b** in phosphate buffer (pH 6.8, $\mu = 0.2$ M).

Table 1 Thermodynamic parameters of interactions between the porphyrin **1b** and DNA[a]

DNA	Temp. (T/°C)	$K_{app}/10^6$	ΔG	ΔH	$\Delta S(-T\Delta S)$[b]
CTDNA	18	3.15	−36.2		
	25	2.26	−36.2		
	32	1.59	−36.2	−34.2	+6.7(−2.0)
	39	1.23	−36.4		
poly(dA-dT)$_2$	18	28.8	−41.6		
	25	10.3	−40.0		
	32	4.02	−38.6	−106.2	−221.8(+66.1)
	39	1.48	−36.9		
poly(dG-dC)$_2$	18	0.38	−31.1		
	25	0.27	−31.0		
	32	0.18	−30.7	−39.0	−27.2(+8.1)
	39	0.13	−30.6		

[a] K_{app} (M^{-1}) is the apparent binding constant of the porphyrin–DNA interaction in phosphate buffer (pH 6.8, $\mu = 0.2$ M). ΔG (kJ mol^{-1}) is the binding free energy calculated from the equation $\Delta G = -RT \ln K_{app}$. The enthalpy ($\Delta H$, kJ mol^{-1}) and entropy (ΔS, J K^{-1} mol^{-1}) changes of the porphyrin–DNA interaction are calculated from the slope ($-\Delta H/R$) and intercept ($\Delta S/R$) of van't Hoff plots of ln K_{app} *versus* $1/T$, respectively. [b] $-T\Delta S$ (kJ mol^{-1}) is calculated at 25 °C (298 K).

Moreover, their interaction is enthalpically driven. The enthalpy changes in the binding of porphyrin **1b** to poly(dA-dT)$_2$ are more negative than those in the binding of porphyrin **1b** to poly(dG-dC)$_2$, suggesting that porphyrin **1b** interacts more strongly with poly(dA-dT)$_2$ than it does with poly(dG-dC)$_2$. In other words, interaction of porphyrin **1b** with DNA is more selective to AT-rich sites than to GC-rich sites.

Conclusions

The absence of two *meso*-substituents at *trans*-positions enables dicationic **1b** to intercalate into DNA, although tetracationic H_2TDMImP is only bound to the outside of DNA due to the four bulky dimethylimidazolium rings. In the intercalation of **1b** into the DNA base pairs, one of the positively charged *N*,*N*′-dimethylimidazolium rings is located in the minor groove near the phosphate backbone and the other is placed in the major groove near the other phosphate backbone. These results show that differences in the structure and number of *meso*-substituents result in changes of DNA-binding properties. This finding is important for our understanding of porphyrin–DNA interactions at a molecular level. Studies on the interaction of metal complexes of **1b** with DNA as well as the characterization of **2b** in solution are currently underway and will be reported elsewhere.

Experimental

A. Materials and instruments

1-Methylimidazole, 1-methylpyrazole, trifluoroacetic acid and iodomethane were purchased from Junsei Chemical Co. Ltd. Pyrrole, paraformaldehyde, chloranil† and methyl fluorosulfonate were obtained from Tokyo Kasei Chemical Co. Ltd. CTDNA, poly(dG-dC)$_2$ and poly(dA-dT)$_2$ were purchased from Sigma Co. Ltd. and were used as received. Pyrrole, 1-methylimidazole and 1-methylpyrazole were distilled under reduced pressure before use. Other chemicals were used as received without further purification and all solvents were of reagent grade. 1-Methylimidazole-2-carbaldehyde,[14a] 1-methylpyrazole-4-carbaldehyde[14b] and 2,2′-dipyrrolylmethane[9c] were prepared according to the literature methods. *meso*-Bisdiazolylporphyrins were synthesized by a slight modification of the Lindsey method.[9] H_2TDMImP was synthesized by the previous method.[8] UV–visible spectra were recorded for solutions at 25 °C (unless otherwise stated) on a JASCO V-570 spectrophotometer equipped with a JASCO ETC-505T temperature controller using 10 mm quartz cells. CD spectra of solutions were recorded on a JASCO J-720 WI spectropolarimeter using 10 mm quartz cells. ^{1}H NMR spectra were recorded at 270 MHz on a JEOL GSX-720 spectrometer or at 300 MHz on a JNM-LA300 spectrometer. Elemental analyses were performed at the Central Laboratory of Faculty of Science and Technology, Keio University and the Shonan Bunseki Center.

B. Synthesis of cationic porphyrins

Synthesis of H_2BMImP (porphyrin 1a). 2,2′-Dipyrrolylmethane (458 mg, 3.1 mmol) and *N*-methylimidazole-2-carbaldehyde (304 mg, 3.1 mmol) were dissolved in 600 cm^3 of freshly distilled dichloromethane. Trifluoroacetic acid (0.150 cm^3, 1.95 mmol) was then added and the mixture was stirred under nitrogen at room temperature for 24 h. Chloranil (974 mg, 3.96 mmol) was added and stirring was continued for 2 h. The mixture was then gently refluxed at 40 °C for 1 h. After neutralization with triethylamine (3 cm^3) at room temperature, the solvent was evaporated to give a pink residue. This was taken up into a minimum amount of dichloromethane and subjected to column chromatography in which a column was packed with neutral active alumina (activity III). Elution with dichloromethane gave a major pink product with two separated bands. Evaporation of the solvent of each fraction followed by recrystallization from dichloromethane–hexane afforded a purple solid (110 mg, 30%). ^{1}H NMR (300 MHz; $CDCl_3$; Me_4Si) δ (a) −3.31 (br s, 2 H, NH), 3.42 (s, 6 H, imidazole 1*N*-CH_3), 7.51 (s, 4 H, imidazole-4H), 7.71 (s, 4 H, imidazole-5H), 9.02 (d, 4 H, pyrrole-βH), 9.41 (d, 4 H, pyrrole-βH), 10.35 (s, 2 H, *meso*-H); (b) −3.30 (br s, 2 H, NH), 3.50 (s, 6 H, imidazole 1*N*-CH_3), 7.52 (s, 4 H, imidazole-4H), 7.72 (s, 4 H, imidazole-5H), 9.03 (d, 4 H, pyrrole-βH), 9.42 (d, 4 H, pyrrole-βH), 10.40 (s, 2 H, *meso*-H); Vis ($CHCl_3$) λ_{max}/nm (log ε) 406 (5.28), 500 (4.11), 535 (3.67), 574 (3.58), 626 (3.59) (Elemental analysis for $C_{28}H_{22}N_8 \cdot 2H_2O$ requires C, 66.39; H, 5.17; N, 22.12. Found: C, 66.86; H, 4.71; N, 22.24%); mp >300 °C.

Synthesis of H_2BDMImP (porphyrin 1b). To 15 mg of H_2BMImP (**1a**) dissolved in 25 cm^3 of dichloromethane was added, 1.5 cm^3 of iodomethane and the mixture was then stirred under nitrogen at 40 °C for 24 h. The precipitate was then filtered off and washed with dichloromethane. Drying of the precipitate under vacuum afforded a dark purple solid (22 mg, 90%). ^{1}H NMR (270 MHz; DMSO-d_6; Me_4Si) δ −3.56 (br s, 2 H, NH), 3.75 (s, 12 H, imidazole 1*N*-CH_3 and 3*N*-CH_3), 8.54 (s, 4 H, imidazole-4H and -5H), 9.27–9.28 (d, 4 H, pyrrole-βH), 9.96–9.98 (d, 4 H, pyrrole-βH), 10.99 (s, 2 H, *meso*-H); Vis (phosphate buffer at pH 6.8, μ = 0.2 M) λ_{max}/nm (log ε) 394 (5.12), 498 (4.01), 534 (4.04), 565 (3.78), 617 (3.87) (Elemental analysis for $C_{30}H_{28}I_2N_8 \cdot 2H_2O$ requires C, 45.59; H, 4.08; N, 14.18. Found: C, 45.59; H, 4.27; N, 14.06%); mp >300 °C.

Synthesis of H_2BMPzP (porphyrin 2a). To 240 cm^3 of freshly distilled dichloromethane were added 2,2′-dipyrrolylmethane (200 mg, 1.35 mmol) and 1-methylpyrazole-4-carbaldehyde (152 mg, 1.35 mmol). Trifluoroacetic acid (0.065 cm^3, 0.85 mmol) was then added and the mixture was stirred under nitrogen at room temperature for 15 h. Chloranil (432 mg, 1.75 mmol) was added and stirring was continued for 2 h. The mixture was then gently refluxed at 40 °C for 1 h. After neutralization with triethylamine at room temperature, the solvent was evaporated off to give a dark pink residue. This was taken up into a minimum amount of dichloromethane and subjected to column chromatography in which a column was packed with silica gel. Elution with dichloromethane using gradient ethyl acetate gave a major pink product. Rechromatography on a column of basic active alumina (activity I) and elution with dichloromethane–hexane 9 : 1 gave a major pink product on the first band. Evaporation of the solvent followed by recrystallization from dichloromethane–hexane afforded a purple solid (70 mg, 22%). ^{1}H NMR (300 MHz; $CDCl_3$; Me_4Si) δ −2.97 (br s, 2 H, NH), 4.37 (s, 6 H, pyrazole-1*N*-CH_3), 8.25 (s, 2 H, pyrazole-5H), 8.40 (s, 2 H, pyrazole-3H), 9.33 (d, 4 H, pyrrole-βH), 9.42 (d, 4 H, pyrrole-βH), 10.30 (s, 2 H, *meso*-H); Vis ($CHCl_3$) λ_{max}/nm (log ε) 411 (5.51), 507 (4.08), 544 (4.02), 580 (3.65), 641 (3.87) (Elemental analysis for $C_{28}H_{22}N_8 \cdot H_2O$ requires C, 68.84; H, 4.95; N, 22.94. Found: C, 69.07; H, 4.79; N, 22.69%); mp >300 °C.

Synthesis of H_2BDMPzP (porphyrin 2b). Into a solution of 30 mg of H_2BMPzP **2a** in 30 cm^3 of dichloromethane was injected 0.1 cm^3 of methyl fluorosulfonate and the mixture was then stirred under argon at room temperature for 27 h. The precipitate was then filtered off, and washed with dichloromethane and subsequently with acetone and cold methanol. Recrystallization from ethanol afforded a purple solid (25 mg, 56%). ^{1}H NMR (300 MHz; DMSO-d_6; Me_4Si) δ −2.97 (br s, 2 H, NH), 4.37 (s, 12 H, pyrazole-1*N*-CH_3 and -2*N*-CH_3), 9.48 (s, 4 H, pyrazole-3H and -5H), 9.55 (d, 4 H, pyrrole-βH), 9.84 (d, 4 H, pyrrole-βH), 10.78 (s, 2 H, *meso*-H); Vis (phosphate buffer at pH 6.8, μ = 0.0 M) λ_{max}/nm(log ε) 399 (5.28), 502 (4.02), 538 (3.88), 566 (3.84), 618 (3.82) (Elemental analysis for

† IUPAC name for chloranil is 2,3,5,6-tetrachloro-1,4-benzoquinone.

$C_{30}H_{28}N_8(FSO_3)_2$ requires C, 51.57; H, 4.04; N, 16.04. Found: C, 51.89; H, 4.09; N, 16.17%); mp >300 °C.

C. Spectral measurements

All experiments, except where specifically indicated, were performed at 25 °C in a phosphate buffer (pH 6.8). The buffer solution consists of 6 mM Na_2HPO_4, 2 mM NaH_2PO_4, 1 mM EDTA and a sufficient amount of NaCl to give a final ionic strength of $\mu = 0.2$ M. A stock solution of calf thymus DNA (CTDNA), poly(dG-dC)$_2$ and poly(dA-dT)$_2$ was prepared and stored in phosphate buffer. Extinction coefficients of $\varepsilon_{260} = 1.31 \times 10^4$ M^{-1} cm^{-1}, $\varepsilon_{254} = 1.68 \times 10^4$ M^{-1} cm^{-1} and $\varepsilon_{262} = 1.32 \times 10^4$ M^{-1} cm^{-1} were used to determine the CTDNA,[15] poly(dG-dC)$_2$[16] and poly(dA-dT)$_2$[17] concentration in base pairs. Porphyrin concentrations were determined spectrophotometrically with $\varepsilon_{394} = 1.32 \times 10^5$ M^{-1} cm^{-1} for **1b** and $\varepsilon_{407} = 1.57 \times 10^5$ M^{-1} cm^{-1} for H_2TDMImP.[8]

Visible absorption spectra were measured on a JASCO V-570 spectrophotometer at a spectral bandpass of 2 nm with 0.5 nm spectral resolution. Wavelength calibration was carried out using a holmium oxide-glass standard. Induced CD spectra were obtained on a carefully calibrated JASCO J-720 WI spectropolarimeter. Wavelength and intensity calibration was carried out using a 0.060% (w/v) aqueous solution of (−)-ammonium camphor-10-sulfonate (Aldrich). CD spectra were recorded with the following instrument parameter settings: 2.0 nm bandwidth, 2.0 s time constant, 0.5 nm step resolution and 200 nm min^{-1} scan speed between 700 to 200 nm. The spectra were obtained from 4 time scans. Typically, porphyrin was titrated by stepwise addition of the concentrated stock solution of DNA directly to 2.5 cm^3 of starting volume of porphyrin solution. Visible and induced CD spectra were measured subsequently after the spectra were stabilized.

Binding constants for the interaction of cationic porphyrins with DNA were determined by absorption spectrophotometric titrations at a certain temperature. The fixed amount of cationic porphyrin in phosphate buffer was titrated at a certain temperature with a stock solution of DNA. The changes in absorbance of the Soret band upon addition of DNA were monitored at the maximum of the Soret band. The apparent binding constant, K_{app}, of cationic porphyrins to DNA was calculated by equation (1).

$$[DNA]_{total}/(|\varepsilon_{app} - \varepsilon_f|) = \{1/(|\varepsilon_b - \varepsilon_f|)\}[DNA]_{total} + 1/\{K_{app}(|\varepsilon_b - \varepsilon_f|)\} \quad (1)$$

where ε_{app}, ε_f and ε_b correspond to A_{obsd}/[porphyrin], the extinction coefficient for the free porphyrin and the extinction coefficient for the porphyrin in the fully bound form, respectively. In the plot of $[DNA]_{total}/(|\varepsilon_{app} - \varepsilon_f|)$ *versus* $[DNA]_{total}$, K_{app} is given by the ratio of the slope to the intercept.[18] The thermodynamics of the porphyrin–DNA interaction was studied in terms of the values of the binding constants determined at various temperatures, *i.e.* in the range 18–39 °C.

D. Measurements of viscosity and melting temperature (T_m)

The viscosity of DNA solutions was measured at 30 ± 1 °C in a temperature-controlled circulating water-bath using an Ubbelohde viscometer. Typically, 10.0 cm^3 of phosphate buffer was transferred to the viscometer to obtain the reading of flow time. For determination of solution viscosity, 10.0 cm^3 of buffered solution of 45 μM DNA was taken to the viscometer and a flow time reading was obtained. An appropriate amount of porphyrin in a buffered solution was then added to the viscometer to give a certain R (= [porphyrin]/[DNA base pair])-value while keeping the DNA concentration constant, and the flow time was read. The flow times of samples were measured after a thermal equilibrium was achieved (*ca.* 60 min). Each point measured was the average of at least five readings with a standard deviation of less than ±1%. The data obtained were presented as (η/η_o) *versus* R, where η is the reduced specific viscosity of DNA in the presence of porphyrin and η_o is the reduced specific viscosity of DNA alone.[12,19]

The melting curves of both free DNA and porphyrin–DNA complex in phosphate buffer were obtained by measuring the hyperchromicity of DNA absorbance at 260, 254, and 262 nm as a function of temperature for CTDNA, poly(dG-dC)$_2$ and poly(dA-dT)$_2$, respectively. Melting temperatures were measured in phosphate buffer solutions pH 6.8 ($\mu = 0.2$ M NaCl) containing 45 μM DNA. The temperature was scanned from 25 to 95 °C at a speed of 2 °C per min. The melting temperature (T_m) was taken as the mid-point of the hyperchromic transition.

Acknowledgements

The research was supported in part by a Grant-in-Aid for Scientific Research (No. 10440199) from the Ministry of Education, Science, Sports, and Culture of the Japanese Government. D. H. T. thanks the Ministry of National Education of the Republic of Indonesia for financial support.

References

1 R. T. Wheelhouse, D. Sun, H. Han, F. X. Han and L. H. Hurley, *J. Am. Chem. Soc.*, 1998, **120**, 3261; I. Haq, J. O. Trent, B. Z. Chowdhry and T. C. Jenkins, *J. Am. Chem. Soc.*, 1999, **121**, 1768; F. X. Han, R. T. Wheelhouse and L. H. Hurley, *J. Am. Chem. Soc.*, 1999, **121**, 3561; E. Izbicka, R. T. Wheelhouse, E. Raymond, K. K. Davidson, R. A. Lawrence, D. Y. Sun, B. E. Windle, L. H. Hurley and D. D. Von Hoff, *Cancer Res.*, 1999, **59**, 639.
2 M. Sirish and H. J. Scheider, *Chem. Commun.*, 1999, 907.
3 G. Pratviel, J. Bernadou and B. Meunier, *Met. Ions Biol. Syst.*, 1996, **33**, 399 and references therein.
4 N. E. Makundan, G. Petho, D. W. Dixon, M. S. Kim and L. G. Marzilli, *Inorg. Chem.*, 1994, **33**, 4676; N. E. Makundan, G. Petho, D. W. Dixon and L. G. Marzilli, *Inorg. Chem.*, 1995, **34**, 3677; J. E. McClure, L. Baudouin, D. Mansuy and L. G. Marzilli, *Biopolymers*, 1997, **42**, 203.
5 R. F. Pasternack and E. J. Gibbs, *Met. Ions Biol. Syst.*, 1996, **33**, 367 and references therein.
6 I. E. Borissevitch and S. C. M. Gandini, *J. Photochem. Photobiol. B: Biol.*, 1998, **43**, 112; D. W. Dixon and V. Steullet, *J. Inorg. Biochem.*, 1998, **69**, 25; M. Sirish and H. J. Scheider, *Chem. Commun.*, 2000, 23.
7 A. B. Guliaev and N. B. Leontis, *Biochemistry*, 1999, **39**, 15425.
8 D. H. Tjahjono, T. Akutsu, N. Yoshioka and H. Inoue, *Biochim. Biophys. Acta*, 1999, **1472**, 333.
9 (*a*) J. S. Lindsey and R. W. Wagner, *J. Org. Chem.*, 1989, **54**, 828; (*b*) Y. Kobuke and H. Miyagi, *J. Am. Chem. Soc.*, 1994, **116**, 4111; (*c*) Q. M. Wang and D. W. Bruce, *Synlett*, 1995, 1267.
10 R. F. Pasternack, P. R. Huber, P. Boyd, G. Engasser, L. Francesconi, E. Gibbs, P. Fasella, G. C. Venturo and L. deC. Hinds, *J. Am. Chem. Soc.*, 1972, **94**, 4511; K. Kano, H. Minamizono, T. Kitae and S. Negi, *J. Phys. Chem. A*, 1997, **101**, 6118.
11 R. Lyng, A. Rodger and B. Nordén, *Biopolymers*, 1991, **31**, 1709; R. Lyng, A. Rodger and B. Nordén, *Biopolymers*, 1992, **32**, 1201.
12 S. Satyanarayana, J. C. Dabrowiak and J. B. Chaires, *Biochemistry*, 1992, **31**, 9319; S. Satyanarayana, J. C. Dabrowiak and J. B. Chaires, *Biochemistry*, 1993, **32**, 2573.
13 M. A. Sari, J. P. Battioni, D. Dupre, D. Mansuy and J. B. Le Pecq, *Biochemistry*, 1990, **29**, 4205.
14 (*a*) P. E. Iversen and H. Lund, *Acta Chem. Scand.*, 1966, **20**, 2649; (*b*) I. L. Finar and G. H. Lord, *J. Chem. Soc.*, 1957, 3314.
15 R. D. Well, J. E. Larson, R. C. Grant, B. E. Shortle and C. R. Cantor, *J. Mol. Biol.*, 1970, **54**, 465.
16 W. Muller and D. M. Crothers, *J. Mol. Biol.*, 1968, **35**, 251.
17 D. E. V. Schmechel and D. M. Crothers, *Biopolymers*, 1971, **10**, 465.
18 A. M. Pyle, J. P. Rehman, R. Meshoyrer, C. V. Kumar, N. J. Turro and J. K. Barton, *J. Am. Chem. Soc.*, 1989, **111**, 3051; J. Onuki, A. V. Ribas, M. H. G. Medeiros, K. Araki, H. E. Toma, L. H. Catalani and P. D. Mascio, *Photochem. Photobiol.*, 1996, **63**, 272; S. Mettath, B. R. Munson and R. K. Pandey, *Bioconjugate Chem.*, 1999, **10**, 94.
19 D. L. Banville, L. G. Marzilli, J. A. Strickland and W. D. Wilson, *Biopolymers*, 1986, **25**, 1837; T. A. Gray, K. T. Yue and L. G. Marzilli, *J. Inorg. Biochem.*, 1991, **41**, 205.